Pergamon

Int. Comm. Heat Mass Transfer, Vol. 25, No. 2, pp. 279–288, 1998
Copyright © 1998 Elsevier Science Ltd
Printed in the USA. All rights reserved
0735-1933/98 $19.00 + .00

PII S0735-1933(98)00015-3

PARTICULATE VISCOUS EFFECTS ON THE COMPRESSIBLE BOUNDARY-LAYER TWO-PHASE FLOW OVER A FLAT PLATE

Ali J. Chamkha
Department of Mechanical and Industrial Engineering
Kuwait University
P. O. Box 5969
Safat, 13060 - Kuwait

(Communicated by J.P. Hartnett and W.J. Minkowycz)

ABSTRACT

The problem of compressible boundary-layer laminar flow of a particulate suspension over a semi-infinite flat plate is solved numerically using the finite-difference methodology. The mathematical model employed includes such effects as particle-phase viscous stresses, variable position-dependent particle slip coefficient, and general power-law viscosity-temperature and thermal conductivity-temperature relations. Graphical results for the displacement thicknesses, skin-friction coefficients, and the wall heat transfer coefficient for both the fluid and particle phases are presented and discussed in detail. In addition, a parametric study is performed to illustrate the influence of the particle to fluid viscosity ratio on the flow properties. © 1998 Elsevier Science Ltd

Introduction

The problem considered in this paper is that of a steady, compressible, laminar, boundary-layer, two-phase (particle-fluid) flow over a semi-infinite flat plate. In addition to its importance as a fundamental problem in fluid-particle dynamics, this problem has possible application in many industries. Examples are fluidized beds, flow over turbine blades, environmental dust storm over deserts, and gas purification. Special cases of this problem have been considered by Singleton [1] and Wang and Glass [2] . Singleton [1] uses a series method and obtains asymptotic solutions for the large-slip region (near the leading edge of the flat plate or surface) and the small-slip region far downstream. Wang and Glass [2] report both asymptotic solutions as well as finite-difference-based numerical results for the whole computational domain. Their asymptotic large-slip solution provided the initial profiles of flow properties

for their numerical finite-difference solution. Investigations on the incompressible version of the present problem have been reported by Osiptsov [3], Prabha and Jain [4], Chamkha and Peddieson [5], and Chamkha [6]. The basic conclusion of the work on the incompressible problem is that a catastrophic growth in the particle-phase wall density suggesting the presence of a singularity predicted somewhere downstream of the plate's leading edge. This singular behavior in the wall density is believed to be related to the particle-phase tangential velocity at the wall which vanishes at the singularity point.

It is of special interest in this paper to investigate whether the singular behavior observed in the problem of incompressible two-phase flow over a semi-infinite plate still exists for the compressible version and to understand the effects of particle-phase viscosity on the flow and heat transfer properties.

Governing Equations

Consider steady, compressible, laminar, boundary-layer two-phase flow in a half space bounded by a semi-infinite flat plate. The plate is coincident with the plane $y = 0$ and the flow is a uniform stream in the plane $y > 0$ parallel to the plate. Far from the plate, both phases are in both hydrodynamic and thermal equilibrium. The particles are all assumed to be of one size and spherical in shape and moving with the same velocity. Besides, there is no radiative heat transfer from one particle to another, chemical reaction, coagulation, phase change, and deposition. The fluid phase is assumed to behave as a perfect gas. The fluid and particles motions are coupled only through drag and heat transfer between them. The drag force is modeled using Stokes linear drag theory and the small particle volume fraction assumption inherent in the dusty-gas model (see, Marble [7]) is retained in this problem. Other interaction forces such as the virtual force (Zuber [8]), the shear lift force (Saffman [9]), and the spin-lift force (Rubinow and Keller [10]) will be neglected compared to the drag force.

The governing equations for this investigation are based on the balance laws of mass, linear momentum, and energy for both phases. The boundary-layer form of the equations can be written as

$$\frac{\partial}{\partial x}(\rho u) + \frac{\partial}{\partial y}(\rho v) = 0 \tag{1}$$

$$\rho\left(u\frac{\partial u}{\partial x} + v\frac{\partial u}{\partial y}\right) = \frac{\partial}{\partial y}\left(\mu\frac{\partial u}{\partial y}\right) + \rho_p N(u_p - u) \tag{2}$$

$$c\rho(u\frac{\partial T}{\partial x} + v\frac{\partial T}{\partial y}) = \frac{\partial}{\partial y}(k\frac{\partial T}{\partial y}) + \mu(\frac{\partial u}{\partial y})^2 + \rho_p N(u_p - u)^2 + c_p \rho_p N_T(T_p - T) \tag{3}$$

$$P = \rho RT \tag{4}$$

$$\frac{\partial}{\partial x}(\rho_p u_p) + \frac{\partial}{\partial y}(\rho_p v_p) = 0 \tag{5}$$

$$\rho_p(u_p\frac{\partial u_p}{\partial x} + v_p\frac{\partial u_p}{\partial y}) = \frac{\partial}{\partial y}(\mu_p\frac{\partial u_p}{\partial y}) - \rho_p N(u_p - u) \tag{6}$$

$$\rho_p(u_p\frac{\partial v_p}{\partial x} + v_p\frac{\partial v_p}{\partial y}) = \frac{\partial}{\partial y}(\mu_p\frac{\partial v_p}{\partial y}) - \rho_p N(v_p - v) \tag{7}$$

$$c_p\rho_p(u_p\frac{\partial T_p}{\partial x} + v_p\frac{\partial T_p}{\partial y}) = \mu_p(\frac{\partial u_p}{\partial y})^2 - c_p\rho_p N_T(T_p - T) \tag{8}$$

where ρ, u, v, P and T represent the fluid-phase density, velocity component in the x-direction, velocity component in the y-direction, pressure, and temperature, respectively. μ, c, k and R are the fluid-phase dynamic viscosity, specific heat, thermal conductivity, and gas constant, respectively. The subscript p refers to the same variable for the particle phase. $N = 18\mu/(\rho_s d^2)$ and $N_T = 12k/(\rho_s d^2 c_p)$ (where ρ_S and d are the density for the particle material and the particle diameter, respectively) are the momentum and temperature transfer coefficients, respectively.

It is seen from Equations (6) through (8) that the particle phase is assumed to have viscous effects which are not present in the models reported by Singleton [1] and Wang and Glass [2]. These effects can model particle-particle interaction and particle-wall interaction. They can also be thought of as a natural consequence of the averaging processes involved in representing a discrete system of particles as a continuum (see, for instance, Drew [11], and Drew and Segal [12]). The particle-phase viscous effects have been investigated by many previous investigators (see, Tsuo and Gidaspow [13] and Gadiraju et al., [14]. Also, the particles are assumed to be dragged along by the fluid and, therefore, have no analog of pressure.

To obtain closure of the governing equations, a knowledge about the dependence of the viscosities of both phases as well as the thermal conductivity of the fluid phase on flow variables is needed. Following Wang and Glass [2], the viscosity of the fluid phase will be assumed to vary with temperature. However,

in the absence of a fundamental theory on how the particle-phase viscosity vary (if so), it will be assumed constant herein as a first approximation.

$$\frac{\mu}{\mu_\infty} = \left(\frac{T}{T_\infty}\right)^\omega, \quad \frac{\mu_p}{\mu_{p\infty}} = 1 \qquad (0.5 \le \omega \le 1.0) \tag{9}$$

where ω is a power index coefficient, T_∞ is the free-stream temperature, and μ_∞ and $\mu_{p\infty}$ are the free-stream fluid- and particle-phase viscosity coefficients, respectively.

The physics of this problem suggests the following boundary conditions:

$$\begin{aligned}
&u(x,0) = 0, \quad v(x,0) = 0, \quad T(x,0) = T_0 \\
&u_p(x,0) = S\frac{\partial u_p}{\partial y}(x,0), \; v_p(x,0) = 0 \\
&u(x,\infty) = U_\infty, \; u_p(x,\infty) = U_\infty, \; v_p(x,\infty) = v(x,\infty) \\
&T(x,\infty) = T_\infty, \; T_p(x,\infty) = T_\infty, \; \rho(x,\infty) = \rho_\infty, \; \rho_p(x,\infty) = \rho_{p\infty} = \kappa\rho_\infty
\end{aligned} \tag{10}$$

where ρ_∞, U_∞, T_0, S, and κ are the free-stream density and velocity, fluid-phase wall temperature, particle-phase wall slip, and the mass loading ratio of particles, respectively. It should be mentioned that the fourth equation in Equations (9) is borrowed from rarefied gas dynamics since the particle phase may behave as a rarefied gas.

Substituting the following modified Blasius transformations (with $\kappa = 1$)

$$\begin{aligned}
&x = U_\infty \xi / (N(1-\xi)), \; y = U_\infty / (N\,\mathrm{Re}_\infty^{1/2})\,(2\xi/(1-\xi))^{1/2}\,\eta \\
&u = U_\infty F, \; v = U_\infty((1-\xi)/(2\xi))^{1/2}\,(G + \eta F)/\mathrm{Re}_\infty^{1/2} \\
&u_p = U_\infty F_p, \; v_p = U_\infty((1-\xi)/(2\xi))^{1/2}\,(G_p + \eta F_p)/\mathrm{Re}_\infty^{1/2} \\
&T = T_\infty H, \; T_p = T_\infty H_p, \; \rho = \rho_\infty Q, \; \rho_p = = \rho_\infty Q_p \\
&\mathrm{Re}_\infty = \rho_\infty U_\infty / (N\mu_\infty), \; \mathrm{Pr} = \mu c / k, \; \mathrm{Ec} = U_\infty^2/(cT_\infty), \; \beta = \mu_{p\infty}/\mu_\infty, \; \gamma = c/c_p
\end{aligned} \tag{11}$$

into Equations (1) through (7) and Equations (9) yields

$$\partial_\eta(QG) + QF + 2\xi(1-\xi)\,\partial_\xi(QF) = 0 \tag{12}$$

$$\begin{aligned}
&H^\omega\,\partial_\eta^2 F + (\omega H^{\omega-1}\partial_\eta H - QG)\partial_\eta F - 2\xi/(1-\xi)((1-\xi)^2 \\
&QF\partial_\xi F - Q_p H^\omega F_p - F)) = 0
\end{aligned} \tag{13}$$

$$H^{\omega}\,\partial_{\eta}^{2}H + (\omega H^{\omega-1}\,\partial_{\eta}H - \mathrm{Pr}\,QG)\,\partial_{\eta}H - 2\xi(1-\xi)\mathrm{Pr}\,QF\,\partial_{\xi}H$$
$$+ \mathrm{Ec}\,\mathrm{Pr}\,H^{\omega}(\partial_{\eta}F)^{2} + 2\xi/(1-\xi)\,(\mathrm{Ec}\,\mathrm{Pr}\,Q_{p}H^{\omega}(F_{p}-F)^{2} + \qquad (14)$$
$$2Q_{p}\,H^{\omega}(H_{p}-H)/3) = 0$$

$$QH = 1 \qquad (15)$$

$$\partial_{\eta}(Q_{p}G_{p}) + Q_{p}F_{p} + 2\xi(1-\xi)\,\partial_{\xi}(Q_{p}F_{p}) = 0 \qquad (16)$$

$$\beta\partial_{\eta}^{2}F_{p} - Q_{p}G_{p}\,\partial_{\eta}F_{p} - 2\xi/(1-\xi)$$
$$((1-\xi)^{2}\,Q_{p}F_{p}\,\partial_{\xi}F_{p} + Q_{p}H^{\omega}(F_{p}-F)) = 0 \qquad (17)$$

$$\beta\,\partial_{\eta}^{2}G_{p} - Q_{p}G_{p}\,\partial_{\eta}G_{p} - \beta\partial_{\eta}^{2}(\eta F_{p}) - \eta Q_{p}G_{p}\,\partial_{\eta}F_{p} + \eta Q_{p}F_{p}^{2}$$
$$-2\xi(1-\xi)Q_{p}F_{p}\,\partial_{\xi}(G_{p}+\eta F_{p}) - 2\xi/(1-\xi)\,Q_{p}H^{\omega}\,(G_{p}-G+\eta(F_{p}-F)) = 0 \qquad (18)$$

$$Q_{P}\,G_{p}\,\partial_{\eta}H_{p} - \beta\,\mathrm{Ec}\gamma\,(\partial_{\eta}F_{p})^{2} + 2\xi(1-\xi)Q_{p}F_{p}\,\partial_{\xi}H_{p}$$
$$+ 4\xi/(1-\xi)\gamma Q_{p}\,H^{\omega}(H_{p}-H)/(3\,\mathrm{Pr}) = 0 \qquad (19)$$

$$F(\xi,0) = 0,\ G(\xi,0) = 0, H(\xi,0) = t_{o},\ F_{p}(\xi,0) = S((1-\xi)/(2\xi))^{1/2}\partial_{\eta}F_{p}(\xi,0)$$
$$G_{p}(\xi,0) = 0,\ F(\xi,\infty) = 1,\ F_{p}(\xi,\infty) = 1, G_{p}(\xi,\infty) = G(\xi,\infty), H(\xi,\infty) = 1, \qquad (20)$$
$$H_{p}(\xi,\infty) = 1,\ Q(\xi,\infty) = 1,\ Q_{p}(\xi,\infty) = 1$$

It is assumed that the wall slip parameter S is a function of the wall position ξ (since the wall slip velocity is related to ξ). A general function of the form

$$S = S_{R}((1-\xi)/\xi)^{r} \qquad (21)$$

(where S_R and r are constants) is employed in the present work. It can be seen that the form of Equation (21) allows perfect particulate slip at $\xi = 0$ followed by approach to no-slip at a rate controlled by the values of S_R and r.

Of practical interest are the fluid- and particle-phase displacement thicknesses, the skin-friction coefficients, and the wall heat transfer coefficient. These are defined respectively as

$$\Delta(\xi) = \int_{o}^{\infty}(1-QF)\,d\eta,\ \Delta_{p}(\xi) = \int_{o}^{\infty}(1-Q_{p}F_{p})d\eta,\ C(\xi) = H(\xi,0)^{\omega}\,\partial_{\eta}F(\xi,0)$$
$$C_{P}(\xi) = \beta\,\partial_{\eta}F_{p}(\xi,0),\ q_{w}(\xi) = H(\xi,0)^{\omega}\,\partial_{\eta}H(\xi,0)/(\mathrm{Ec}\,\mathrm{Pr}) \qquad (22)$$

Results and Discussion

A numerical solution of Equations (12) through (20) is pursued since no closed-form solution can be found. The tri-diagonal, implicit, iterative, finite-difference method discussed by Blottner [15] is extended to two-phase flow and successfully applied to the problem under consideration.

All first-order derivatives with respect to ξ are represented by three-point backward difference formulas. All second-order differential equations in η are discretized using a three-point central difference quotients while all first-order differential equations in η are discretized using the trapezoidal rule. The computational domain was divided into 1001 nodes in the ξ direction and 195 nodes in the η direction. Since it is expected that most changes in the boundary layer occur in the vicinity of the wall, variable step sizes in η are utilized with $\Delta\eta_1 = 0.001$ and a growth factor of 1.03. Also, constant small step sizes in ξ with $\Delta\xi = 0.001$ are used. The governing equations are then converted into sets of linear tri-diagonal algebraic equations which are solved by the Thomas Algorithm (see, Blottner [15]) at each iteration. The convergence criterion required that the difference between the current and the previous iterations be 10^{-5}. It should be mentioned that many numerical experimentations were performed by altering the step sizes in both directions to ensure accuracy of the results and to assess grid independence. Many results were obtained throughout the course of this work. A representative set is presented in figures 1 through 6 to show the effects of the viscosity ratio β on the solutions. In all these figures $S_R = 50$ and $r = 1$.

Figures 1 through 3 show the development of the displacement thicknesses of both phases Δ and Δ_p, the fluid-phase skin-friction coefficient C, and the particle-phase skin-friction coefficient C_p along the flat plate for various values of β, respectively. At $\xi = 0$, the drag force between the phases is maximum

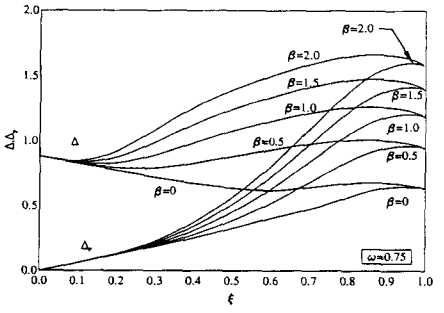

FIG. 1
Fluid and Particle-Phase Displacement Thicknesses Profiles

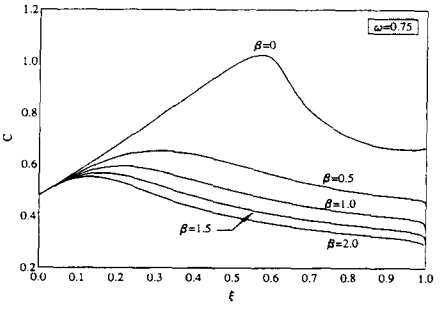

FIG. 2
Fluid-Phase Skin Friction Coefficient Profiles

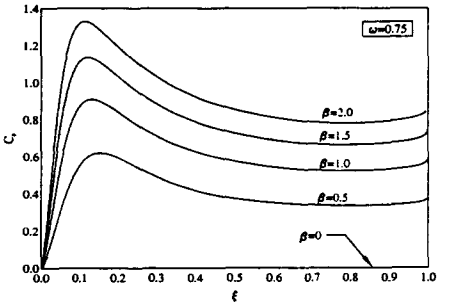

FIG. 3

Particle-Phase Skin Friction Coefficient Profiles

and it decreases as ξ increases until it vanishes at $\xi = 1$ where equilibrium between the phases exists. This momentum exchange mechanism causes the fluid-phase displacement thickness to decrease (which causes an increase in the fluid-phase skin friction) and the particle-phase displacement thickness to increase until equilibrium is reached. However, as β increases the effective viscosity of the mixture increases causing a rapid increase in the values of Δ as the flow moves downstream toward equilibrium. It should be noted that the particle-phase streamlines are completely unaffected by the fluid-phase displacement at $\xi = 0$. This is because of the frozen condition (where both phases move independently) existing there. These behaviors are evident from figure 1. As β increases, the domain of particle-phase viscous effects increases causing an increase in the region close to the wall where significant deviations from uniformity occur. This results in increases in the values of Δ and Δ_p and decreases in the values of C as shown in figures 1 and 2. In addition, the values of C_p shown in figure 3 increases as β increase since C_p is directly proportional to β.

Figures 4 and 5 depict the effects of the wall particle-phase tangential velocity and density profiles at the wall, respectively. The transition from a perfect slip condition at $\xi = 0$ to a no-slip condition downstream at about $\xi \geq 0.6$ is shown in figure 4. Figure 5 shows that for an inviscid particle phase ($\beta = 0$) the particle-phase wall density becomes large in the vicinity of $\xi = 0.5$. This behavior was also observed for the case of incompressible flow (see, Ospitsov [3] and Chamkha and Peddieson [5]). However, in the present work a continuous solution for $Q_p(\xi,0)$ is predicted in the entire range $0 \leq \xi \leq 1$ unlike the incompressible case where no continuous solutions existed. The peak value of $Q_p(\xi,0)$ for $\beta = 0$ is large and falls outside the range of the figure. It has a value of about 200 occurring at $\xi = 0.6$ and approaches the equilibrium conditions at $\xi = 1$ without going below unity. This indicates that a particle-free zone (discussed below) does not exist for $\beta = 0$. It is seen that as the particulate slip decreases, lower peaks in $Q_p(\xi,0)$ are predicted. However, for $\beta > 0$ (viscous particle phase) $Q_p(\xi,0)$ vanishes over a

big region far from the leading edge of the plate and then approaches the equilibrium conditions at $\xi = 1$.

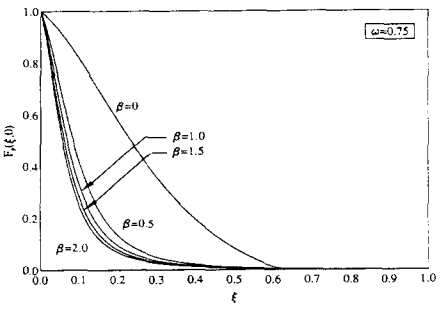

FIG. 4
Wall Particle-Phase Tangential Velocity Profiles

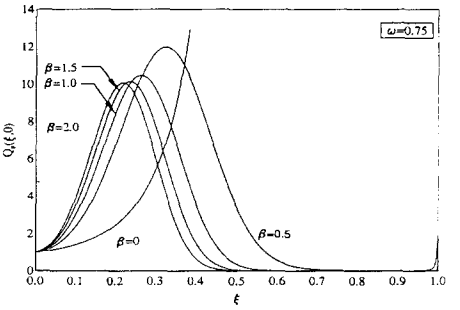

FIG. 5
Wall Particle-Phase Density Profiles

The vanishing of $Q_p(\xi,0)$ is suggestive of the formation of a particle-free zone at the wall somewhere downstream. This phenomenon has been predicted by the work of Young and Hanratty [16]. It is seen from figure 5 that as β increases the peaks in the $Q_p(\xi,0)$ profiles move toward the leading edge of the plate and the particle-free region increases.

Figure 6 illustrates the changes in the wall heat transfer coefficient q_w as the viscosity ratio β is altered. It is seen that a sharp peak in the values of q_w (corresponding to the peak in $Q_p(\xi,0)$) exits for $\beta = 0$ and this peak moves upstream and its value decreases as β increases. The behavior of q_w, C, and C_p with respect to ξ observed in figures 2 ,3, and 6 is a property of relaxation-type problems.

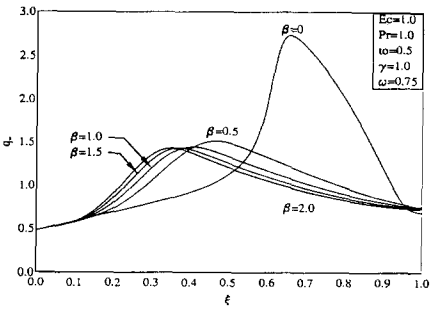

FIG. 6
Wall Heat Transfer Coefficient Profiles

It should be mentioned that some adjustments were made in the computer program and results for the incompressible case were obtained. These special case results were in excellent agreement with those

reported by Chamkha and Peddieson [5, 17]. The velocity and temperature fields reported by Wang and Glass [2] were also compared with the present results and were found to be in good agreement. These comparisons gave some confidence in the numerical procedure. No comparisons with experimental data were made since these data are lacking at present.

Conclusion

The problem of steady, compressible, laminar, boundary-layer flow of a particulate suspension over a flat plate was formulated using a generalized dusty-gas model allowing for particulate viscous effects and solved numerically using the finite difference method. Important flow and heat transfer characteristics of the problem were reported and discussed. A parametric study was performed to show the effects of the particle-phase viscosity on the solutions. In contrast with the incompressible version of the current problem, it was found that continuous solutions existed throughout the computational domain. Another major prediction of the present work was that for a viscous particle phase a particle-free zone was formed at the plate surface. This prediction could not be verified by experimental data due to the absence of such data at present. Favourable comparisons with previously published results on special cases of this problem were made which gave confidence in the accuracy of the numerical method. It is hoped that the present results be of use for environmental agencies in validating computer routines and serve as a stimulus for experimental work on the present problem.

Acknowledgments

The author wishes to thank the Research Administration at Kuwait University for funding the work presented in this paper under grant number EPM 079. Also, thanks are due to Engineer Khalil Khanafer for preparing the graphs used in this manuscript.

References

1. R.E. Singleton, *Zamp* **16,** 421 (1965).

2. B.Y. Wang, and I.I. Glass, *Journal of Fluid Mechanics* **186,** 223 (1988).

3. A.N. Osiptsov, *Fluid Dynamics* **15,** 512 (1980).

4. S. Prabha, and A.C. Jain, *Applied Scientific Research* **36,** 81 (1980).

5. A.J. Chamkha and J. Peddieson, *Developments in Theoretical and Applied Mechanics* **16**, II-4 (1992).

6. A.J. Chamkha, *Developments in Theoretical and Applied Mechanics* **16**, II-4. 24 (1992).

7. F.E. Marble, *Annual Review of Fluid Mechanics* **2**, 297 (1970).

8. N. Zuber, *Chemical Engineering Sciences* **19**, 897 (1964).

9. P.G. Saffman, *Journal of Fluid Mechanics* **22**, 385 (1965).

10. S.I. Rubinow, and J.B. Keller, *Journal of Fluid Mechanics* **11**, 447 (1961).

11. D.A. Drew, *Annual Review of Fluid Mechanics* **15**, 261 (1983).

12. D.A. Drew, and L.A. Segal, *Studies in Applied Mathematics* **50**, 233 (1971).

13. Y.P. Tsuo, and D. Gidaspow, *AIChE Journal* **36**, 88 (1990).

14. M. Gadiraju, and et al., *Mechanics Research Communications* **19**, 7 (1992).

15. F.G. Blottner, *AIAA Journal* **8**, 193 (1970).

16. J.B. Young, and T.J. Hanratty, *AIChE Journal* **37**, 1529 (1991).

17. A.J. Chamkha and J. Peddieson, *Computational Mechanics and Experimental Measurements* **15**, (1991) 25.

Received November 20, 1997